ELSEVIER

Biochimica et Biophysica Acta 1320 (1997) 65–72

BIOCHIMICA ET BIOPHYSICA ACTA
BBA

^{1}H, ^{13}C and ^{17}O isotropic and anisotropic hyperfine coupling prediction for the tyrosyl radical using hybrid density functional methods

Patrick J. O'Malley, Darryl Ellson

Department of Chemistry, University of Manchester Institute of Science and Technology, Manchester, M60 1QD, UK

Received 11 December 1996; accepted 23 January 1997

Abstract

Hybrid density functional calculations are used to directly calculate the principal hyperfine tensor values for ^{1}H, ^{13}C and ^{17}O in two models of the tyrosyl radical, *p*-methylphenoxyl and *p*-ethylphenoxyl. Both hydrogen bonded and non-hydrogen bonded phenoxyl radicals are studied. A comparison is made between calculated values and those obtained from experimental EPR and ENDOR studies. Outstanding agreement between experiment and theory is observed.

Keywords: Tyrosyl radical; EPR; Electron nuclear double resonance; Isotropic hyperfine coupling; Anisotropic hyperfine coupling

1. Introduction

Electron transfer in biology is usually associated with metal centres or cofactors such as quinones or flavins. Only quite recently have amino acid residues been implicated in such a role[1,2].

Tyrosyl radicals have been studied experimentally in Photosystem II [3], ribonucleotide reductase [4], prostaglandin synthase [5], galactose oxidase [6] and amine oxidase [7]. Magnetic resonance techniques such as Electron Paramagnetic Resonance (EPR) and Electron Nuclear DOuble Resonance (ENDOR) spectroscopies have been the principal methods used to investigate the electronic structure of the radicals involved.

A complimentary approach is to calculate the electronic structure using high level electronic structure methods based on semiempirical, ab initio Hartree Fock or density functional methods. Semiempirical methods have been used by us to calculate the geometry of the tyrosyl radical [8]. While the geometry prediction is excellent the direct calculation of isotropic and anisotropic hyperfine couplings is poor and resort must be made to indirect methods based on spin densities combined with McConnell or McConnell Strathdee methods [8]. Good agreement can be observed for the ^{1}H isotropic couplings by use of the INDO method providing a suitable geometry is used [9]. The ^{17}O and ^{13}C values are poorly predicted however. The more rigorous ab initio Hartree Fock based methods are particularly poor at dealing with free radical properties [9,10]. Density functional methods have been shown to give impressive results for a wide range of molecular properties and preliminary results have indicated that free radical properties can be predicted to high accuracy using hybrid density functional methods [10–12]. For these reasons

Abbreviations: B3LYP, Becke3 Lee Yang Parr; INDO, intermediate neglect of differential overlap; EPR, electron paramagnetic resonance; ENDOR, electron nuclear double resonance; PM3, parameter method 3; HOMO, highest occupied molecular orbital.

PII S0005-2728(97)00013-3

our calculations on the tyrosyl radical have concentrated on such hybrid methods.

Free radicals are best characterised by their hyperfine structure due to the magnetic interaction of the unpaired electron spin density with the nuclear magnetic moments. The EPR powder pattern is usually too broad to allow resolution of hyperfine terms. This can be overcome by resort to ENDOR methods which have been successfully used to obtain proton hyperfine tensors for the tyrosyl radical in a number of species [3,4]. Recently isotopic enrichment with ^{13}C combined with EPR spectral simulation has been used to obtain ^{13}C hyperfine tensor information for the tyrosyl radical [13].

For calculation purposes the 3×3 hyperfine interaction tensor can be separated into its isotropic (spherically symmetric) and anisotropic (dipolar) components. To first order isotropic hyperfine interactions, $A_{\mathrm{iso}}(N)$ are related to the spin densities, $\rho^{s}(r_N)$, at the corresponding nuclei by:

$$A_{iso}(N) = (8\pi/3)\, g_e g_N \beta_N \beta_e \rho^{s}(r_N)$$

The anisotropic components are derived from the classical expression of interacting dipoles:

$$A_{ij}(N) = g_{\mathrm{e}} g_N \beta_N \beta_{\mathrm{e}} \sum P_{\mu\nu}^{\alpha-\beta} \langle \varphi_\mu | r_{kN}^{-5} \left(r_{kN}^2 \delta_{ij} - 3 r_{kNi} r_{kNj} \right) | \varphi_\nu \rangle$$

The isotropic component can be obtained form the Fermi contact analysis given by most modern electronic structure programmes. The anisotropic components can be obtained from the spin only electric field gradient tensors. Experimentally in the solid state the total tensor, i.e., isotropic plus anisotropic is observed. For the tyrosyl radical powder ENDOR studies have been used to obtain the hydrogen total principal hyperfine tensor values from the turning points in the ENDOR spectral envelope [3,4]. For ^{13}C and ^{17}O, EPR studies combined with isotopic enrichment have been used [4,13].

2. Methods

All calculations were performed with the electronic structure program Gaussian 94. The hybrid functional B3LYP was used combined with the EPR-III basis set [10]. The geometry of the radicals was first optimised at the PM3 level.

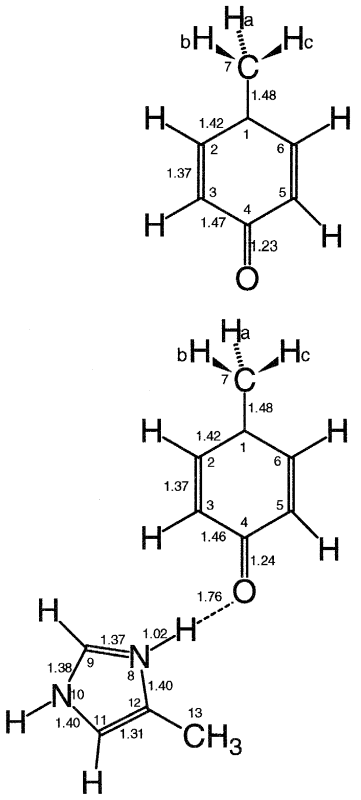

Fig. 1. Structure, numbering scheme and optimised bond distances, in Ångstroms (10^{-10} m), for the methylphenoxyl radical and its hydrogen bonded complex with methylimidazole.

The methyl phenoxyl radical was used as a model of the tyrosyl radical (Fig. 1). Extension of the model to the ethyl phenoxyl structure produced no change in the ring hyperfine couplings confirming that extension beyond a methyl group produces no change in the hyperfine coupling constants. As such the methylphenoxyl radical is an ideal, computationally efficient, model for the tyrosyl radical. A hydrogen bonded complex of this radical with an imadazole ring was used to model the effect of hydrogen bonding (Fig. 1). In Photosystem II a histidine residue is believed to hydrogen bond to the Y_D tyrosyl radical and hence this model is a particularly good simulation of the environment of Y_D in Photosystem II. The optimised bond distances are also shown in Fig. 1. All hyperfine couplings are given in gauss (G); 1 G = 0.1 mT.

3. Results and discussion

Table 1, Tables 2 and 3 gives the calculated hyperfine coupling constants for the non-hydrogen bonded and hydrogen bonded phenoxyl radical and compares them with those obtained from EPR and ENDOR measurements.

Significant changes are predicted to occur in going from a non-hydrogen bonded to a hydrogen bonded radical. In general a reduction in the hyperfine coupling values is noted on going to the hydrogen bonded situation. The largest change occurs for the C4 position. The experimental data are clearly in excellent agreement with the calculated couplings for the hydrogen bonded complex. For ^{13}C (Table 1) and ^{17}O (Table 3) couplings the agreement is outstanding. Any major disagreement that occurs lies in the smaller components of the coupling tensors. Experimentally these have been obtained via spectral simulations [4,13] which will be mainly influenced by the largest

Table 1
[^{13}C]Hyperfine coupling constants (G) for the *p*-methylphenoxyl radical and the hydrogen bonded complex of Fig. 1

	p-Methylphenoxyl (calculated)			H-Bond complex (calculated)			Tyrosyl [a] (experimental)	
	isotropic	anisotropic	total	isotropic	anisotropic	total	isotropic	total
		T_{11}	**A_{11}**		**T_{11}**	**A_{11}**		**A_{11}**
		T_{22}	**A_{22}**		**T_{22}**	**A_{22}**		**A_{22}**
		T_{33}	**A_{33}**		**T_{33}**	**A_{33}**		**A_{33}**
C1	12.7	−11.8	0.9	12.2	−11.8	0.3	10.0	−2.0
		−11.2	1.4		−11.3	0.8		−2.0
		23.0	35.6		23.2	35.4		34.0
C2	−9.2	−6.3	−15.6	−8.2	−4.6	−12.8	−8.5	−10.5
		2.8	−6.4		2.0	−6.2		−8.5
		3.5	−5.7		2.6	−5.6		−6.5
C3	8.0	−8.3	−0.3	6.3	−7.2	−0.9	3.0	−5.0
		−7.9	0.1		−6.7	−0.4		−5.0
		16.1	24.1		14.0	20.4		19.0
C4	−12.1	−3.4	−15.5	−8.8	−1.7	−10.5	−8.9	−10.0
		0.6	−11.5		0.0	−8.8		−9.8
		2.8	−9.3		1.8	−7.0		−6.8
C5	8.0	−8.3	−0.3	6.5	−7.3	−0.7	3.0	−5.0
		−7.9	0.1		−6.8	−0.3		−5.0
		16.1	24.1		14.0	20.6		19.0
C6	−9.2	−6.3	−15.6	−8.4	−5.2	−13.6	−8.5	−10.5
		2.8	−6.4		2..3	−6.1		−8.5
		3.5	−5.7		2.9	−5.5		−6.5
C7	−5.1	−0.6	−5.6	−5.0	−0.7	−5.7	N/D	N/D
		0.2	−5.0		0.0	−5.1		
		0.4	−4.7		0.7	−4.3		
C9	N/A	N/A	N/A	0.0	−0.1	−0.1	N/D	N/D
					0.0	0.0		
					0.1	0.1		
C11	N/A	N/A	N/A	0.0	0.0	−0.1	N/D	N/D
					0.0	−0.1		
					0.1	0.0		
C12	N/A	N/A	N/A	0.0	−0.1	−0.1	N/D	N/D
					−0.1	−0.1		
					0.1	0.1		
C13	N/A	N/A	N/A	0.0	−0.1	−0.1	N/D	N/D
					−0.1	−0.1		
					0.1	0.1		

[a] [13], N/A, not applicable; N/D, not determined.

tensor component. The smaller ones are naturally less accurately determined by such methods. The isotropic values reported in [13] for the 3 and 5 carbon positions are likely to be in error due to incorrect estimation of the smaller tensor components. The theoretically predicted isotropic coupling for these positions

Table 2
[^{1}H]hyperfine coupling constants (G) for the *p*-methylphenoxyl radical and the hydrogen bonded complex

	p-Methylphenoxyl (calculated)			H-Bond complex (calculated)			Tyrosyl [a,b] (experimental)	
	isotropic	anisotropic	total	isotropic	anisotropic	total	isotropic	total
		$\mathbf{T_{11}}$	$\mathbf{A_{11}}$		$\mathbf{T_{11}}$	$\mathbf{A_{11}}$		$\mathbf{A_{11}}$
		$\mathbf{T_{22}}$	$\mathbf{A_{22}}$		$\mathbf{T_{22}}$	$\mathbf{A_{22}}$		$\mathbf{A_{22}}$
		$\mathbf{T_{33}}$	$\mathbf{A_{33}}$		$\mathbf{T_{33}}$	$\mathbf{A_{33}}$		$\mathbf{A_{33}}$
H2	2.8	−1.1	1.7	2.0	−1.1	1.2	1.6	−
		−0.3	2.5		−0.1	1.9		1.6
		1.4	4.1		1.2	3.2		2.6
H3	−7.4	−3.5	−10.9	−6.6	−3.2	−9.8	−6.6	−9.8
		−0.8	−8.2		−0.8	−7.3		−6.9
		4.3	−3.2		4.0	−2.5		−2.9
H5	−7.4	−3.5	−10.9	−6.7	−3.2	−9.9	−6.6	−9.1
		−0.8	−8.2		−0.8	−7.5		−7.3
		4.3	−3.2		4.0	−2.6		−2.9
H6	2.8	−1.1	1.7	2.3	−1.1	1.2	1.6	−
		−0.3	2.5		−0.2	2.1		1.6
		1.4	4.1		1.2	3.5		2.6
H7a	25.9	−1.0	24.9	29.6	−1.1	28.4	N/D	N/D
		−0.4	25.5		−0.4	29.1		
		1.4	27.4		1.6	31.2		
H7b	6.5	−0.7	5.7	9.7	−0.9	8.9	N/D	N/D
		−0.6	5.9		−0.5	9.2		
		1.3	7.8		1.4	11.1		
H7c	6.5	−0.7	5.7	5.0	−0.8	4.2	N/D	N/D
		−0.6	5.9		−0.5	4.5		
		1.3	7.8		1.3	6.4		
H8	N/A	N/A	N/A	0.0	−1.5	−1.4	−	−1.1
					−1.2	−1.2		−1.1
					2.7	2.8		−
H9	N/A	N/A	N/A	0.0	−0.2	−0.2	N/D	N/D
					0.2	−0.2		
					0.4	0.4		
H10	N/A	N/A	N/A	0.0	−0.1	−0.1	N/D	N/D
					−0.1	−0.1		
					0.1	0.1		
H11	N/A	N/A	N/A	0.0	−0.1	−0.1	N/D	N/D
					−0.1	−0.1		
					0.1	0.1		
H13a	N/A	N/A	N/A	0.0	−0.1	−0.1	N/D	N/D
					−0.1	−0.1		
					0.3	0.3		
H13b	N/A	N/A	N/A	0.0	−0.2	−0.2	N/D	N/D
					−0.2	0.2		
					0.4	0.4		
H13c	N/A	N/A	N/A	0.0	0.0	−0.1	N/D	N/D
					0.0	−0.1		
					0.1	0.0		

[a] [3], [b] [18]. N/A, not applicable; N/D, not determined.

Table 3
^{17}O and ^{14}N hyperfine coupling constants (G) for the *p*-methylphenoxyl radical and the hydrogen bonded complex

	p-Methylphenoxyl (calculated)			H-Bond complex (calculated)			Tyrosyl [a] (experimental)	
	isotropic	anisotropic	total	isotropic	anisotropic	total	isotropic	total
		$\mathbf{T_{11}}$	$\mathbf{A_{11}}$		$\mathbf{T_{11}}$	$\mathbf{A_{11}}$		$\mathbf{A_{11}}$
		$\mathbf{T_{22}}$	$\mathbf{A_{22}}$		$\mathbf{T_{22}}$	$\mathbf{A_{22}}$		$\mathbf{A_{22}}$
		$\mathbf{T_{33}}$	$\mathbf{A_{33}}$		$\mathbf{T_{33}}$	$\mathbf{A_{33}}$		$\mathbf{A_{33}}$
O	−9.1	20.3	11.2	−9.1	17.2	8.1	−10.2	4.4
		20.2	11.1		17.0	7.8		4.4
		−40.4	−49.5		−34.2	−43.4		−39.5
N8	N/A	N/A	N/A	−0.3	0.0	−0.4	N/D	N/D
					0.0	−0.4		
					0.0	−0.3		
N10	N/A	N/A	N/A	0.0	0.0	0.0	N/D	N/D
					0.0	0.0		
					0.0	0.0		

[a] [4], N/A, not applicable; N/D, not determined.

is in good agreement with the value of 8.1 G reported for phenoxyl radicals in solution [14]. Taking these considerations into account, the agreement between experiment and theoretical calculation is very impressive.

The ring proton tensors have been determined quite accurately using powder ENDOR methods. The 3,5 protons are particularly well characterised. They do not show great variation from species to species. In some cases where the radical is not locked in to a rigid hydrogen bond an average value is observed for the two slightly inequivalent protons [4]. The agreement between the calculated values for the hydrogen bonded complex and experimentally determined values is again impressive (Table 2).

For the 2,6 protons only two principal values can be reliably detected from powder ENDOR spectroscopy [3,4]. As Table 2 shows the agreement between theoretical calculation and experiment is good although not as impressive as for the 3,5 protons. We believe that the principal cause for disagreement here may lie in the overestimation of the isotropic (contact term) for these protons. They are attached to a carbon atom which is at a nodal alpha HOMO position (Fig. 2). The contact interaction therefore arises due to a complex network of spin polarisation traversing a number of bonds. This is likely to be difficult to model with high accuracy.

The H7 protons receive spin density via hyperconjugation and vary depending on the extent of overlap with the alpha HOMO situated on the ring system, Fig. 2 and Fig. 3. The extent of this overlap, and hence the ensuing isotropic hyperfine coupling depends on the C6-C1-C7-C8 dihedral angle (ϕ), Fig.

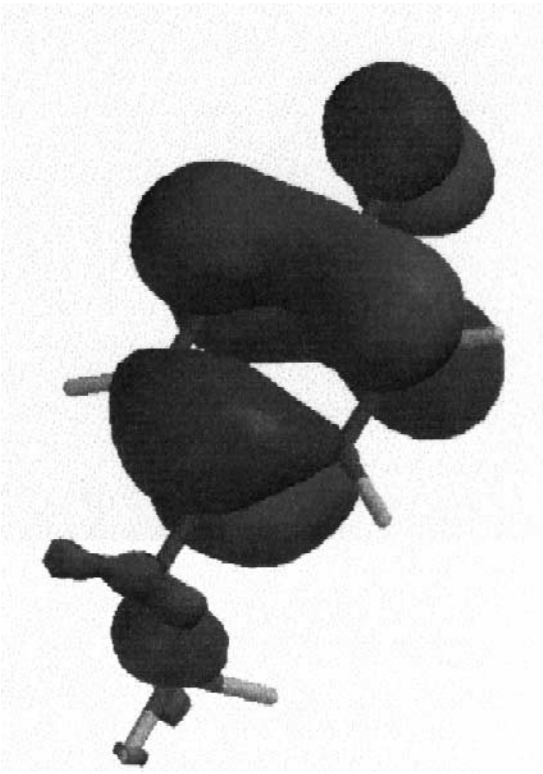

Fig. 2. Alpha highest occupied molecular orbital for the ethylphenoxyl radical. The orientation of the radical is as shown in Fig. 3.

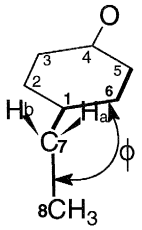

ϕ = 43; Ha = 21.6G, 19.8G,19.2G
Hb = 3.8G, 2.0G, 1.9G

ϕ = 66; Ha = 14.3G, 12.1G, 12.5G
Hb = 1.7G, -0.1G, -0.2G

Fig. 3. Schematic representation of the dihedral angle C8, C7, C1, C6 (ϕ). Principal hyperfine coupling values for ϕ equal to 43° and 66° are given for comparison with experimental determinations in RNR and TYR.HCl. In many of the previous EPR based studies the 'dihedral' angle between the methylene protons, H7a, H7b and the 'p_z' orbital on C1 have been used. Such angles cannot be determined from the X-ray crystal structure studies directly. Assuming a perfectly tetrahedral structure around C7 they can be derived from the ϕ value. For ϕ = 43° the derived methylene proton angles are 13° and 107°, whereas for ϕ = 66°, the methylene proton values are derived as 36° and 84°.

3. A variety of hyperfine couplings and hence dihedral angles are observed for the tyrosyl free radical in different species [3,4] leading to a variety of powder EPR lineshapes. The participation of these protons in the alpha HOMO for the ethyl phenoxyl radical is clearly shown in Fig. 2. For ϕ values of 0° and 90° both hydrogens contribute equally to the alpha HOMO. For dihedral angles of 30° we expect maximum participation from one of the hydrogens (maximum overlap with alpha HOMO) and for dihedral angles of 60° we expect minimum contribution from one of the hydrogens (in plane of ring, no participation in ring alpha HOMO is possible). Previous studies have estimated unpaired spin densities at the C1 carbon atom and used a McConnell type relation combined with a dependance on dihedral angle to explain such couplings [3,4]. While such procedures have been useful in explaining qualitatively the hyperfine couplings of such protons there is always the uncertainty of the unpaired spin density value as well as the McConnell type constant to use. The confusion which can naturally arise form such approximations is well demonstrated in the recent discussion of these couplings in [4]. With our current method we are however able to predict *directly* the hyperfine coupling for such protons as a function of dihedral angle without the need to invoke empirical parameters. Fig. 4 shows a plot of the dependence of the total hyperfine couplings for these protons as a function of the above dihedral angle value. Equal hyperfine coupling values for both protons at 0° and 90°, maximum

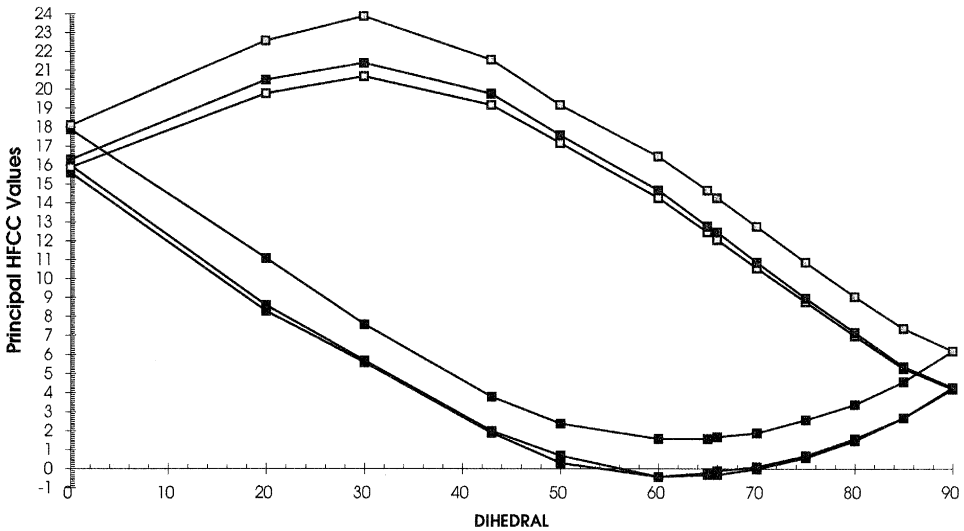

Fig. 4. Plot of dihedral angle (ϕ), see Fig. 3, as a function of the calculated principal hyperfine coupling values of the beta protons H7a (top) and H7b (bottom).

coupling at 30° and minimum coupling at 60° are obtained. To test the quantitative accuracy of hybrid density functional calculations for such couplings we have chosen two tyrosyl radicals where the hyperfine coupling and the dihedral angle value are known experimentally. These correspond to the tyrosyl radical present in tyrosine hydrochloride single crystals (Tyr · HCl) and the tyrosyl radical present in RNR. For the Tyr · HCl radical single crystal structure determination gives a ϕ angle value of 66° [15]. Fassenella and Gordy [16] recorded a value of 14.0 ± 0.5 G for the larger proton isotropic coupling. This is in excellent agreement with the 13 G value obtained from our calculations for this dihedral angle value, see Fig. 3. For the RNR radical, the X-ray crystal structure of the diamagnetic protein [17] gives a value of 43° for ϕ. For this dihedral angle value our calculated couplings (Fig. 3) are 21.6, 19.8 and 19.2 G for the larger proton coupling. The experimentally determined values obtained using powder ENDOR are 21.8, 19.2 and 19.2 G [4]. In this experimental study [4] assignments were also made to the smaller proton couplings. These assignments are extremely difficult to assign experimentally due to the congested nature of small proton couplings. The assignments made in [4] for these smaller coupling values should be reinvestigated in light of the values given in Fig. 3. Clearly where accurate, unambiguous, experimental data is available the agreement between theory and experiment is outstanding. The plot shown in Fig. 4 can be justifiably used to determine the dihedral angle value where only the beta proton hyperfine coupling data is available. This is clearly the case for the tyrosyl, Y_D, radical present in Photosystem II. Here the principal hyperfine coupling values of the larger proton coupling have been accurately determined to be 9.8, 9.1 and 9.1 G for spinach [3]. From Fig. 4 these correspond to a ϕ value of 75°.

Hydrogen bonding of Y_D, one of the tyrosyl radicals present in Photosystem II, to a nearby histidine residue has also been proposed and a hydrogen bond has been detected using powder ENDOR spectroscopy [18]. Only the axial component of the tensor has been observed at 1.1G. As seen from Table 2 this is again excellently predicted by theory. Significant hyperfine coupling is also predictd to ocur at the N8 atom of the imadazole ring (Table 3) which should be detectable experimentally in the Y_D Photosystem II radical.

It is clear therefore that the principal hyperfine tensor values for the tyrosyl radical in vivo can be quantitatively predicted from first principles using hybrid density functional methods. Combined with previous successes for such methods [11,12] they are clearly poised to contribute significantly to our understanding of hyperfine interactions for free radicals and to become an invaluable aid in the assignment of EPR and ENDOR spectral features. The availability of an accurate wavefunction for the unpaired electron should also contribute to a more thorough and fundamental understanding of electron transfer in biological systems.

References

[1] Debus, R.J., Barry, B.A., Babcock, G.T. and McIntosh, L. (1988) Proc. Natl. Acad. Sci. USA 85, 427–430.

[2] Wagner, A.F.V., Frey, M., Neugerbaur, F.A. and Schafer, W. (1992) Proc. Natl. Acad. Sci. USA 89, 996–1000.

[3] Rigby, S.E.J., Nugent, J.H.A and O'Malley, P.J. (1994) Biochemistry 33, 1734–1741.

[4] Bender, C.J., Sahlin, M., Babcock, G.T., Barry, B.A., Chandrashekar, T.K., Salowe, S.P., Lindstrom, B., Peterson, L., Ehrenberg, A. and Sjoberg, B.-M. (1989) J. Am. Chem. Soc. 111, 8076–8092Hoganson, C.W., Sahlin, M., Sjoberg, B.-M. and Babcock, G.T. (1996) J. Am. Chem. Soc. 118, 4672–4679.

[5] Smith, W.L., Eling, T.E., Kulmacz, R.J., Marrott, L.J. and Tsai, A.L. (1992) Biochemistry 31. 3–7.

[6] Whittaker, M.M and Whittaker, J.W. (1990) J. Biol. Chem. 265, 9610–9613.

[7] Jones, S.M., Mu, D., Wemms, D., Smith, A.J., Kaus, S., Maltby, D., Burlingame, A.L. and Kinman, J.P. (1990) Science 248, 981–987.

[8] O'Malley, P.J., MacFarlane, A.J., Rigby, S.E.J. and Nugent, J.H.A. (1995) Biochim Biophys Acta 1232, 175–179.

[9] O'Malley, P.J. and MacFarlane, A.J. (1992) J. Mol. Structure (THEOCHEM) 277, 293–300.

[10] Adamo, C., Barone, V. and Fortunelli, A. (1995) J. Chem. Phys. 102, 384–390.

[11] O'Malley, P.J. and Collins, S.J. (1996) Chem. Phys. Lett. 259, 296–300.

[12] O'Malley, P.J. and Ellson, D.A. (1996) Chem. Phys. Lett. 260, 492–498.

[13] Hulsebosch, R.J., van den Brink, J.S., Hoff, A.J., Nieuwenhuis, S.A.M., Raap, J. and Lugtenburg, J. (1995) Photosynthesis: From Light to Biosphere, Vol. II, P. Mathis (ed.), Kluwer Academic Publishers, Dordrecht, pp. 255–258.

[14] Kirste, B. (1982) J. Magn. Res. 62, 242–250.

[15] Frey, M.N., Koetzle, T.F., Lehmann, M.S., Hamilton, W.C. (1973) J. Chem. Phys. 58, 2547–2556.
[16] Fasanella, E.L., Gordy, W. (1969) Proc. Natl. Acad. Sci (USA) 62, 299–304.
[17] Nordlund, P., Eklund, H. (1993) J. Mol. Biol. 232, 123–133.
[18] Diner, B.A., Tang, X.-S., Zheng, M., Dismukes, G.C., Force, D.A., Randall, D.W and Britt, R.D. (1995) Photosynthesis: From Light to Biosphere, Vol. II, P. Mathis (ed.), Kluwer Academic Publishers, Dordrecht, pp. 200–203.